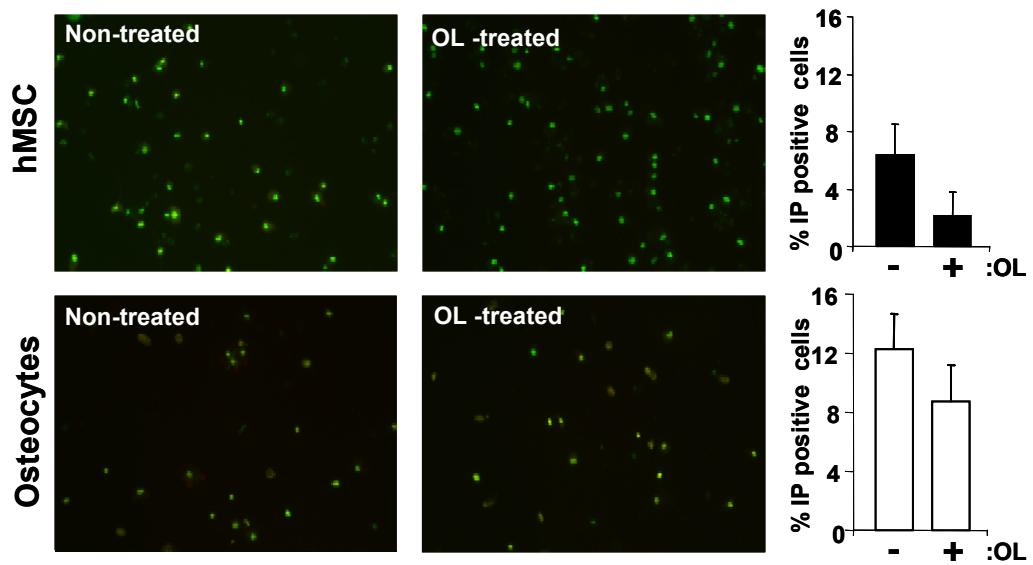


## Supporting Information.

### Degradation of IF1 controls energy metabolism during osteogenic differentiation of stem cells

María Sánchez-Aragó<sup>1</sup>, Javier García-Bermúdez<sup>1</sup>, Inmaculada Martínez-Reyes<sup>1</sup>, Fulvio Santacatterina<sup>1</sup> and José M. Cuezva<sup>1, \*</sup>

#### Supporting Results



**Figure S1. Oligomycin (OL) treatment has no effect on cell death in hMSCs and osteocytes.** Cells were exposed to 6  $\mu$ M OL or left untreated. Cells were double-stained with Hoechst 33342 (green) and propidium iodide (PI, red) and visualized using fluorescence microscopy at 20x magnification. The percentage of PI positive cells (dead cells) was determined by examination of 10 different fields taken at random. Histograms are the means  $\pm$  S.E.M.

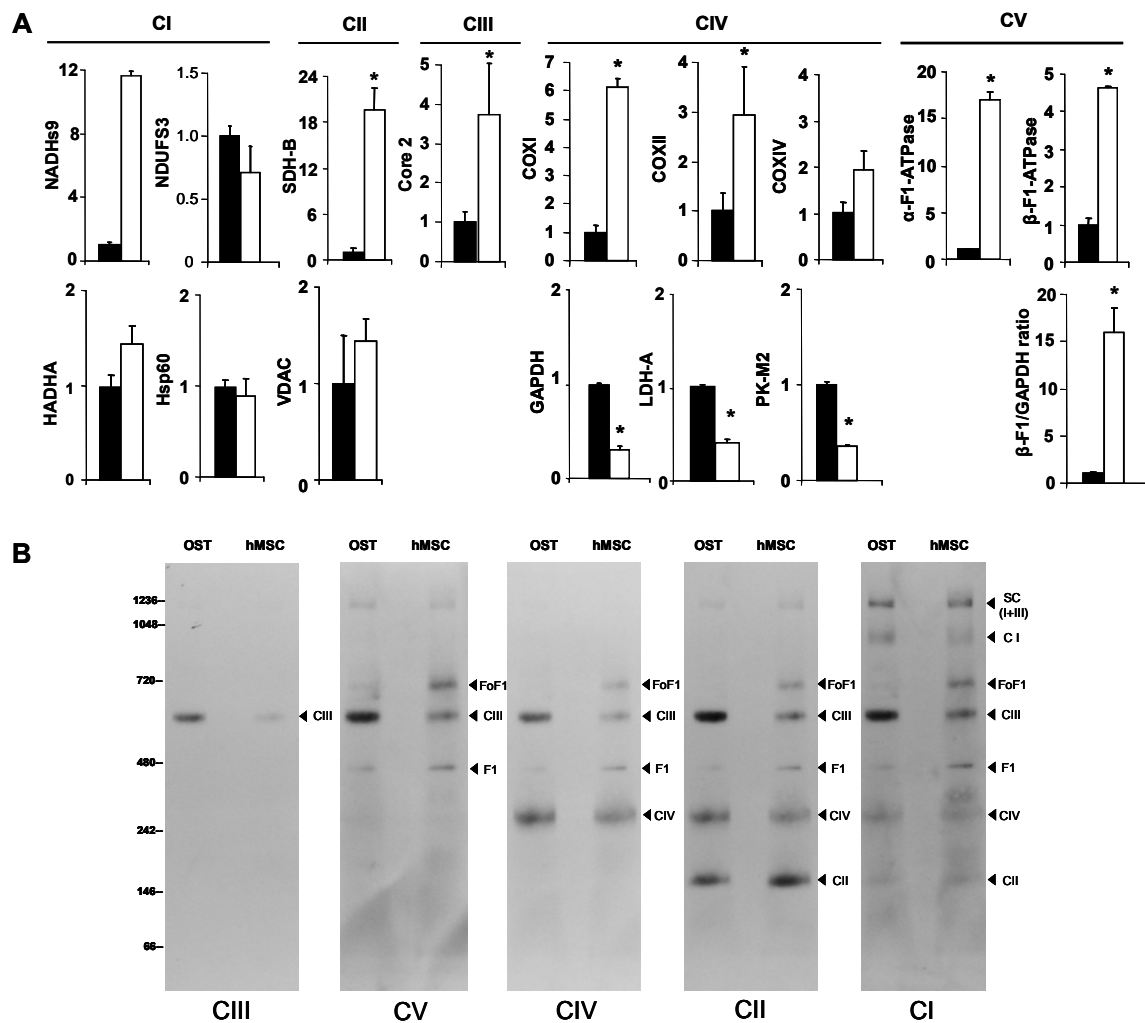


**Figure S2. Differentiation of mitochondria upon osteogenic induction.** **A.** Histograms show the quantification of the expression of mitochondrial (NADHs9, NDUFS3, SDH-B, Core 2, COXI, COXII, COXIV,  $\alpha$ -F1-ATPase,  $\beta$ -F1-ATPase, HADHA, Hsp60 and VDAC) and glycolytic (GAPDH, LDH-A and PK-M2) enzymes in hMSCs (closed bars) and osteocytes (open bars) (for representative blots see Fig. 2A). The bioenergetic signature ( $\beta$ -F1/GAPDH ratio) in hMSCs and osteocytes is also shown. Data are expressed as fold change relative to the values in hMSCs. Bars represent the mean  $\pm$  S.E.M. of four different preparations. \*,  $p < 0.05$  when compared to hMSCs. **B.** Analysis of OXPHOS complexes by BN-PAGE in the presence of *n*-dodecyl  $\beta$ -D-maltoside from digitonin-enriched mitochondrial membranes from hMSC and osteocytes (OST). A representative experiment is shown. The membrane has been sequentially blotted with antibodies against complex III (CIII), complex V (FoF1), complex IV (CIV), complex II (CII) and complex I (CI). The migration of F1-ATPase (F1), supercomplex I+III (SC I+III) and of molecular mass markers (kDa) is also indicated.

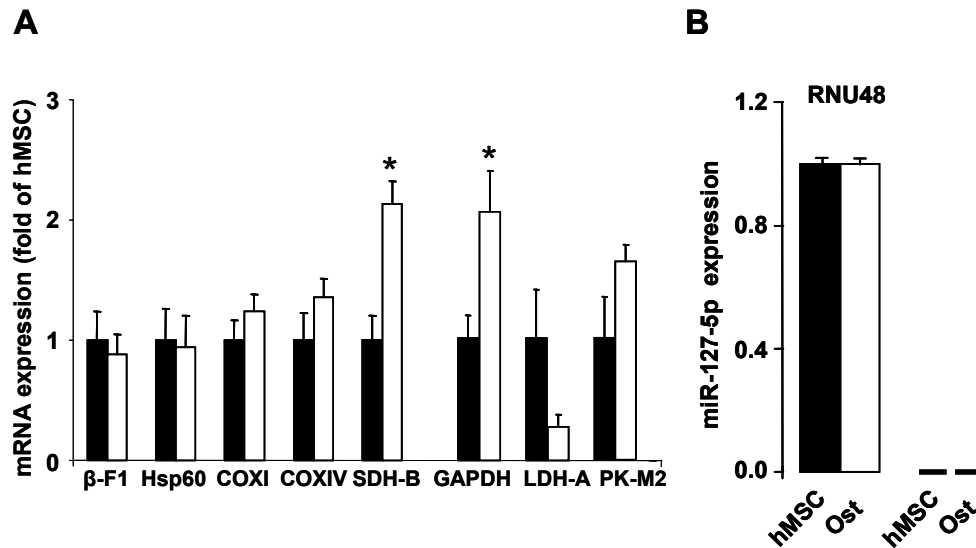


**Figure S3. Post-transcriptional regulation of mitochondrial differentiation.** Total RNA was extracted from hMSC (closed bars) and osteocytes (open bars). **(A)** Expression of representative mitochondrial ( $\beta$ -F1-ATPase, Hsp60, COXIV, COXI, and SDH-B) and glycolytic (GAPDH, LDH-A and PK-M2) mRNAs was assessed by RT-qPCR. Histograms show the mean  $\pm$  S.E.M. of six different determinations. \*,  $p < 0.05$  when compared to hMSCs. **(B)** Quantification of miR-127-5p by RT-qPCR in hMSCs and osteocytes. RNU48 values are shown to highlight the negligible expression of miR-127-5p in both undifferentiated and differentiated cells. Bars are the mean  $\pm$  S.E.M. of 3 independent determinations.

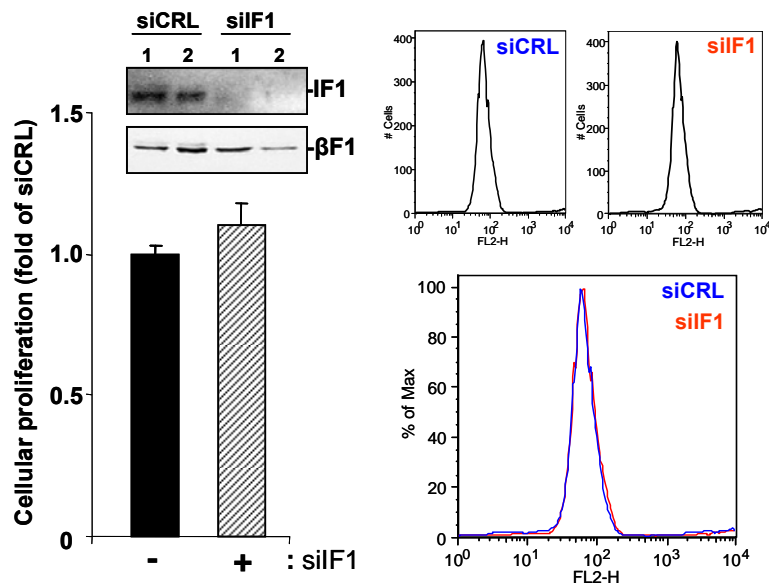


**Figure S4. IF1 is not signaling cellular proliferation in hMSC.** hMSCs were transfected with control (siCRL, closed bars) or siF1 siRNA (siF1, hatched bars) to regulate the expression of IF1. Cellular proliferation was assessed by the incorporation of EdU into cellular DNA. Blue (Control, siCRL) and red (siF1) traces are shown. Bars are the mean  $\pm$  S.E.M. of 6 independent determinations. Data are shown as fold change relative to the values in siCRL cells.

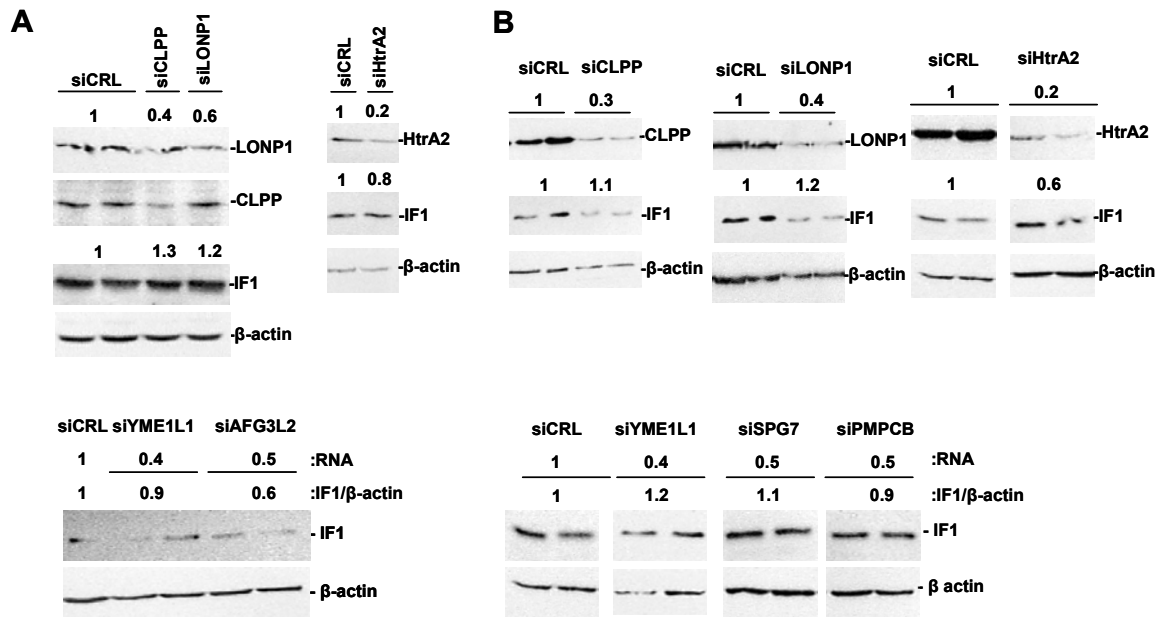


**Figure S5. siRNA screening for the putative protease involved in the degradation of IF1.** hMSCs (A) and HCT116 colon cancer cells (B) were transfected for 48 hours with 80-100 nM siCRL or with the specified siRNA for the following mitochondrial proteases: AFG3L2, CLPP, HtrA2, LONP1, PMPCB, SPG7 and YME1L1. Representative blots of IF1 and  $\beta$ -actin are shown. The calculated IF1/ $\beta$ -actin ratio is indicated on top of the blots. Silencing of CLPP, HtrA2 and LONP1 was verified by western blotting and the degree of silencing indicated on top of the blots. Silencing of AFG3L2, PMPCB, SPG7 and YME1L1 was verified by RT-qPCR and indicated.

## Supporting Methods

**Osteogenic induction and treatments.** To induce osteogenic differentiation, hMSCs were incubated in the osteogenic media containing dexamethasone, ascorbate, Mesenchymal Cell Growth Supplement, L-glutamine, penicillin/streptomycin and  $\beta$ -glycerophosphate (Lonza). For inhibition of mitochondrial serine-proteases, hMSC and osteocytes were treated with 400 $\mu$ M of 4-(2-aminoethyl) benzenesulfonyl fluoride hydrochloride (AEBSF) for the indicated time.

**Antibodies used:** anti-CD44 (1:1,000) from Millipore; anti- $\beta$ -F1-ATPase (1: 25,000) [1]; anti-IF1 (1:200) [2]; anti-PK-M2 (pyruvate kinase M2) (1:1000); anti-NADHs9 (NADH dehydrogenase subunit 9) (1:1,000); anti-GAPDH (1:20,000); anti-LDH-A (1:1,1000) [3]; anti-Hsp60 (Heat Shock Protein) (Stressgene SPA-807, 1:2,000); anti-SDH-B (succinate dehydrogenase subunit B) (1:500) and anti-COXIV (cytochrome c

oxidase subunit IV (1:250) from Invitrogen; anti- $\alpha$ -F1-ATPase ( $\alpha$ -F1-ATPase) (1:1,000) from Molecular Probes; anti-osteopontin (1:1,000), anti-NDUFS3 of complex I (1:1,000), anti-Core 2 of complex III (1:500), anti-MTCO2 (cytochrome c oxidase subunit II) (1:500), anti-MTCO1 (cytochrome c oxidase subunit I) (1:100), anti-VDAC1 (porin) (1:500), anti-LONP1 antibody (1:250) and anti-CLPP (1:200) from Abcam; anti-Htra2/Omi (1:500) from Cell Signaling; anti-tubulin (1:5,000) and anti- $\beta$ -actin (1:100,000) from Sigma. Peroxidase-conjugated anti-mouse and anti-rabbit IgGs (Nordic Immunology, 1: 3,000) were used as secondary antibodies. The blots were developed using the ECL reagent. Quantification of the immunoreactive bands was accomplished using a Kodak DC120 Zoom digital camera and the Kodak 1D Image Analysis Software for Windows. The ratios  $\beta$ -F1-ATPase/Hsp60 and  $\beta$ -F1-ATPase/GAPDH were taken as respective indexes of the bioenergetic competence of the organelle (mitochondrial differentiation) and of the overall mitochondrial activity in the cell (that results from both mitochondrial proliferation and differentiation), and illustrate the two main pathways that restrain the bioenergetic activity of mitochondria in cancer cells [1, 4].

**siRNA silencing.** Transfections were performed using Lipofectamine and Plus Reagent (Invitrogen™). Suppression of IF1 (Qiagen S100908075) expression was exerted by small interfering RNA (siRNA). An inefficient siRNA sequence, Silencer® Select Negative Control #1 plasmid (Ambion/Applied Biosystems), was used as a control. Suppression of expression of mitochondrial proteases was exerted using the following Silencer Select siRNAs (Invitrogen): LONP1 (s17903), CLPP (s15686), HTRA2 (s653), AFG3L2 (s21516), SPG7 (s224671), PMPCB (s18239), YME1L1 (s21077). Silencer Negative Control siRNA #1 (AM4636) was used as control. Silencing was verified by western blotting (LONP1/CLPP/HTRA2) or by RT-qPCR (AFG3L2/SPG7/PMPCB/YME1L1). The forward (F) and reverse (R) primers used were:  $\beta$ -actin, F: 5'- CCAACCGCGAGAAGATGA-3', R: 5'- CCAGAGGCGTACAGGGATAG-3'; PMPCB, F: 5'- TGCCAGCTTGCTGTTTAATG-3', R: 5'-TTGCCTCTTTTATGGAAATGG-3'; YME1L1, F: 5'-CATGGTGGCAGGTGCTTAT-3', R: 5'- CTCCATCTCCCAGGCTCA-3'; SPG7, F: 5'-GTCCGGCTTCTCCAACAC-3', R: 5'- AGGGTAGCTGGTCAAGAGAGG-3'; AFG3L2, F: 5'- GAGGAAGAGGCAACTTTGGA-3', R: 5'-AATGACGACATTTGTTGTTGTATTTAAA-3'.

**Immunohistochemistry.** Formalin-fixed, paraffin-embedded normal and tumor 5  $\mu\text{m}$  sections of human colon and prostate biopsies were used (Origene). Sections were deparaffined and the antigens retrieved by incubation in EDTA for 45 min at 155°C. The monoclonal anti-IF1 (1:200) antibody was used as detailed [5]. Sections were counterstained with hematoxylin.

**Immunofluorescence microscopy.** For co-localization studies, deparaffinated normal human colon and prostate 5  $\mu\text{m}$  tissue sections were used. The primary antibodies used were anti-CD44 (1:50) and anti-IF1 (1:50) [2]. Slides were incubated for 2h in the dark with anti-(rabbit) and anti-(mouse) IgGs conjugated to Alexa Fluor® 488 and 555, respectively. Cellular fluorescence was analyzed by confocal microscopy in a LSM510 META (Zeiss).

**Gene expression analysis by RT-qPCR.** Total RNA was extracted from cell cultures using TRIzol Reagent (Invitrogen) or RNeasy Mini Kit (QIAGEN). RNA was quantified with a Nanodrop ND-1000 spectrophotometer. RNA integrity was assessed with an Agilent 2100 Bioanalyzer. Reverse transcription (RT) reactions were performed using 1  $\mu\text{g}$  of total RNA and the High Capacity Reverse Transcription Kit (Applied Biosystems) with random primers, following manufacturer's instructions. Real-time PCR was performed using Power Sybr Green PCR Master Mix with an ABI PRISM 7900HT instrument (Applied Biosystems). The expression level of indicated mRNAs was determined according to the  $\Delta\Delta\text{Ct}$  method using  $\beta$ -actin as internal control.

**Assessment of cellular proliferation.** The incorporation of 5-ethynyl-2'-deoxy-uridine (EdU) into cellular DNA was determined using the Click-iT EdU Flow Cytometry Assay Kit (Molecular Probes) [5].

**Cell death assays.** Cells were harvested, washed with PBS and incubated in the dark for 5 min with Hoechst 33342 (1mg/mL) and propidium iodide (1mg/mL) solutions. After washing, samples were observed under a Leica DM-IRB fluorescence microscope (UV). The percentage of dead (red staining) cells was calculated from 10 different randomly selected fields for each condition assayed.

**Blue native electrophoresis (BN)-PAGE.** Enriched mitochondrial fractions were isolated from cell cultures using digitonin [6]. Protein extracts were solubilized in BN-loading buffer (1.5 M 6-aminocaproic acid, 50 mM Bis-Tris/HCl pH 7.0) in the presence of 2  $\mu\text{l}$  PMSF/0.5 mM DMSO. *n*-dodecyl  $\beta$ -D-maltoside at the concentration of 3 g/g protein was added to the samples and incubated on ice for 10 min. Solubilized samples were centrifuged for 30 min at 30,000 rpm at 4°C, and the supernatant was

combined with 2  $\mu$ l of sample buffer (500 mM aminocaproic acid, 50 mM Bis-Tris/HCl pH 7.0, 0.5 mM EDTA, 5% Serva Blue G-250) prior to loading in 3-13% gradient gels [7].

### Supporting References

1. Cuezva JM *et al* (2002) The bioenergetic signature of cancer: a marker of tumor progression. *Cancer Res* **62**: 6674-6681
2. Sanchez-Cenizo L, Formentini L, Aldea M, Ortega AD, Garcia-Huerta P, Sanchez-Arago M, Cuezva JM (2010) Up-regulation of the ATPase inhibitory factor 1 (IF1) of the mitochondrial H<sup>+</sup>-ATP synthase in human tumors mediates the metabolic shift of cancer cells to a Warburg phenotype. *J Biol Chem* **285**: 25308-25313
3. Acebo P *et al* (2009) Cancer abolishes the tissue type-specific differences in the phenotype of energetic metabolism. *Transl Oncol* **2**: 138-145
4. Cuezva JM, Ortega AD, Willers I, Sanchez-Cenizo L, Aldea M, Sanchez-Arago M (2009) The tumor suppressor function of mitochondria: translation into the clinics. *Biochim Biophys Acta* **1792**: 1145-1158
5. Formentini L, Sánchez-Aragó M, Sánchez-Cenizo L, Cuezva JM (2012) The mitochondrial ATPase Inhibitory Factor 1 (IF1) triggers a ROS-mediated retrograde pro-survival and proliferative response. *Mol Cell* **45**: 731-742
6. Calvaruso MA, Smeitink J, Nijtmans L (2008) Electrophoresis techniques to investigate defects in oxidative phosphorylation. *Methods* **46**: 281-287
7. Schagger H (2003) Membrane Protein Purification and Crystallization: A Practical Guide. Elsevier Science, USA.